Alternative splicing of N- and C-termini of a *C. elegans* ClC channel alters gating and sensitivity to external Cl^- and H^+

Jerod Denton[1], Keith Nehrke[2], Eric Rutledge[1], Rebecca Morrison[1] and Kevin Strange[1]

[1] *Departments of Anaesthesiology, Pharmacology, and Molecular Physiology and Biophysics, Vanderbilt University Medical Center, Nashville, TN 37232, USA*

[2] *Department of Medicine, Nephrology Unit, University of Rochester Medical Center, Rochester, NY 14642, USA*

CLH-3 is a meiotic cell cycle-regulated ClC Cl^- channel that is functionally expressed in oocytes of the nematode *Caenorhabditis elegans*. CLH-3a and CLH-3b are alternatively spliced variants that have identical intramembrane regions, but which exhibit striking differences in their N- and C-termini. Structural and functional studies indicate that N- and C-terminal domains modulate ClC channel activity. We therefore postulated that alternative splicing of CLH-3 would alter channel gating and physiological functions. To begin testing this hypothesis, we characterized the biophysical properties of CLH-3a and CLH-3b expressed heterologously in HEK293 cells. CLH-3a activates more slowly and requires stronger hyperpolarization for activation than CLH-3b. Depolarizing conditioning voltages dramatically increase CLH-3a current amplitude and induce a slow inactivation process at hyperpolarized voltages, but have no significant effect on CLH-3b activity. CLH-3a also differs significantly in its extracellular Cl^- and pH sensitivity compared to CLH-3b. Immunofluorescence microscopy demonstrated that CLH-3b is translationally expressed during all stages of oocyte development, and furthermore, the biophysical properties of the native oocyte Cl^- current are indistinguishable from those of heterologously expressed CLH-3b. We conclude that CLH-3b carries the oocyte Cl^- current and that the channel probably functions in nonexcitable cells to depolarize membrane potential and/or mediate net Cl^- transport. The unique voltage-dependent properties of CLH-3a suggest that the channel may function in muscle cells and neurones to regulate membrane excitability. We suggest that alternative splicing of CLH-3 N- and C-termini modifies the functional properties of the channel by altering the accessibility and/or function of pore-associated ion-binding sites.

(Received 8 August 2003; accepted after revision 15 October 2003; first published online 17 October 2003)

Corresponding author K. Strange: Vanderbilt University Medical Center, T-4202 Medical Center North, Nashville, TN 37232-2520, USA. Email: kevin.strange@vanderbilt.edu

Members of the ClC superfamily of voltage-gated Cl^- channels are present in all phyla (Jentsch *et al.* 2002). The channels play key roles in diverse and fundamental physiological processes including regulation of skeletal muscle membrane excitability (Adrian & Bryant, 1974; Pusch, 2002) and cytoplasmic Cl^- levels (Staley *et al.* 1996), transepithelial Cl^- transport (Uchida, 2000), acidification of intracellular vesicles (Gunther *et al.* 1998; Mohammad-Panah *et al.* 2003), acid resistance in bacteria (Iyer *et al.* 2002), regulation of nitrate content in plants (Geelen *et al.* 2000) and cation homeostasis in yeast (Gaxiola *et al.* 1998). Nine ClC genes have been identified in mammals and mutations in five of these give rise to inherited muscle, bone, kidney and neurological diseases (Jentsch *et al.* 2002; Haug *et al.* 2003).

Six ClC-type anion channel encoding genes termed *clh-1–6* or *ceclc-1–6* are present in the *C. elegans* genome (Bargmann, 1998; Schriever *et al.* 1999; Nehrke *et al.* 2000). The six nematode ClC channels are representative of the three major subfamilies of mammalian ClCs. We demonstrated recently that *C. elegans* oocytes functionally express a ClC channel encoded by *clh-3* (Rutledge *et al.* 2001). The biophysical properties and regulation of CLH-3 resemble those of mammalian ClC-2 (reviewed in Strange, 2002; Strange, 2003). CLH-3 is activated during oocyte meiotic cell cycle progression, a process termed meiotic maturation, and in response to oocyte swelling (Rutledge *et al.* 2001). Activation occurs by serine/threonine dephosphorylation, mediated by the type-1 protein phosphatases

 DOI: 10.1113/jphysiol.2003.053165

CeGLC-7α/β (Rutledge *et al.* 2002). Meiotic maturation-induced activation of CLH-3 may function to synchronize oocyte cell cycle progression with ovulation and fertilization (Rutledge *et al.* 2001; Rutledge *et al.* 2002; Strange, 2002).

Two CLH-3 splice variants termed CLH-3a and CLH-3b have been cloned from *C. elegans* (Schriever *et al.* 1999; Nehrke *et al.* 2000). These proteins have identical intramembrane domains, but differ significantly in their N- and C-termini. The major differences include a 71 amino acid N-terminal extension on CLH-3a and a 261 amino acid extension of the CLH-3b C-terminus (Fig. 1).

Recent X-ray crystal structure studies of bacterial ClCs indicate that members of this channel family are comprised of intracellular amino (N)- and carboxyl (C)-termini and 18 α-helical domains, 17 of which are intramembrane (Dutzler *et al.* 2002). Dutzler *et al.* (2002) noted that the C-terminus of the *Salmonella enterica* ClC participates in Cl^- coordination within the channel's selectivity filter. They postulated that this interaction provides a structural basis for regulating channel function via cytoplasmic processes. Consistent with this idea, Fong *et al.* (1998) showed that replacement of the most C-terminal 290 amino acids of ClC-0 with the corresponding region of ClC-2 prevented slow gating. In addition, replacement of a shorter C-terminal region of ClC-0 with the analogous region in ClC-1 caused a shift in the apparent voltage sensitivity of the channel and induced current attenuation following hyperpolarizing prepulses (Fong *et al.* 1998).

The intracellular N-terminus has also been proposed to function in channel gating. Mutagenesis studies by Jordt & Jentsch (1997) on ClC-2 suggested that the N-terminus plays a role in activation of the channel by cell swelling, voltage and external H^+. Although the idea has been challenged recently (Varela *et al.* 2002), Gründer *et al.* (1992) proposed that the N-terminus functions as a 'ball' that normally blocks the channel pore via a 'ball-and-chain' type mechanism, analogous to that of voltage-dependent K^+ channels (e.g. Zagotta *et al.* 1990). A splice variant of ClC-2 with a 10 amino acid deletion in the N-terminus has altered voltage-dependent inactivation kinetics (Cid *et al.* 2000). Similarly, N-terminal splice variation of ClC-3 alters voltage-dependent inactivation in addition to channel rectification (Shimada *et al.* 2000).

Given the implied roles of cytoplasmic domains in regulating ClC function, we postulated that the striking differences in the N- and C-termini of CLH-3a and CLH-3b would give rise to channels with distinct gating characteristics and physiological functions. To begin testing this idea, we characterized the biophysical properties of the splice variants expressed heterologously in HEK293 cells. Cell swelling and membrane hyperpolarization activated both channels. However, CLH-3a exhibited unique voltage-dependent characteristics and sensitivity to extracellular Cl^- and H^+ that was not observed in CLH-3b. The functional properties of heterologously expressed CLH-3b were identical to those of the native Cl^- current in the *C. elegans* oocyte. Immunofluorescence studies using CLH-3b-specific antiserum demonstrated that the channel is expressed in the oocyte plasma membrane. These results indicate that the cell cycle-regulated oocyte Cl^- current is probably carried by CLH-3b. Our findings also suggest that the N- and/or C-termini of CLH-3 participate in voltage-dependent gating and influence the channel sensitivity to external Cl^- and H^+. The differences in functional properties of CLH-3a and CLH-3b suggest that the two channels probably play unique physiological roles in *C. elegans*.

Methods

C. elegans strains

Wild type N2 (Bristol) and a *clh-3* deletion mutant strain, *clh-3*(*ok763*), were cultured at 16°C using standard methods (Brenner, 1974).

Transient expression of CLH-3 splice variants

HEK293 (human embryonic kidney) cells were cultured in Eagle's minimal essential medium (MEM; Gibco, Gaithersburg, MD) containing 10% heat-inactivated fetal bovine serum (Gibco), 50 U ml^{-1} penicillin and 50 μg ml^{-1} streptomycin. Cells grown in 35 mm dishes to approximately 50% confluency were transfected using Superfect reagent (Qiagen, Valencia, CA) with either 2 μg green fluorescent protein (GFP) cDNA ligated into pcDNA3, or 1 μg GFP cDNA and 5–6 μg CLH-3a (kindly provided by T. Jentsch) or CLH-3b (Nehrke *et al.* 2000) cDNA ligated into pCDNA3.1. Cells were transfected for 3 h, washed three times with MEM and incubated overnight at 37°C.

Isolation of *C. elegans* oocytes

C. elegans gonads were isolated by placing worms in egg buffer (118 mM NaCl, 48 mM KCl, 2 mM $CaCl_2$, 2 mM $MgCl_2$, 25 mM Hepes, pH 7.3, 340 mOsm) and cutting them behind the pharyngeal bulb and in front of the spermatheca using a 26-gauge needle. Isolated

gonads were transferred to a patch clamp bath chamber mounted on the stage of an inverted microscope. Late-stage oocytes spontaneously released from the cut end of the gonad were used for patch clamp studies. As described previously (Rutledge *et al.* 2001), oocytes undergoing meiotic maturation were identified by the presence of an off-centre nucleus and by the disappearance of the nuclear envelope.

Whole-cell patch clamp recording

HEK293 cells were patch clamped ∼24 h after transfection. Two hours before initiating electrophysiological experiments, the transfected cells were dissociated by brief exposure to trypsin and then plated onto poly L-lysine-coated cover slips. Plated cover slips were placed in a bath chamber mounted on the stage of an inverted microscope. Cells were visualized by fluorescence and differential interference contrast (DIC) microscopy.

Transfected cells were identified by GFP fluorescence and patch clamped using a bath solution containing 90 mM *N*-methyl-D-glucamine chloride (NMDG-Cl) or 90 mM NaCl, 5 mM $MgSO_4$, 1 mM $CaCl_2$, 12 mM Hepes, 8 mM Tris, 5 mM glucose, 80 mM sucrose and 2 mM glutamine (pH 7.4, 295 mOsm), and a pipette solution containing 116 mM NMDG-Cl, 2 mM $MgSO_4$, 20 mM Hepes, 6 mM CsOH, 1 mM EGTA, 2 mM ATP, 0.5 mM GTP, and 10 mM sucrose (pH 7.2, 275 mOsm). Low NaCl solutions were prepared by isosmotic substitution of NaCl for sucrose. Cells were swollen by exposure to a hypotonic (225 mOsm) bath solution that contained no added sucrose.

Oocytes were patch clamped using a bath solution containing 116 mM NMDG-Cl, 2 mM $CaCl_2$, 2 mM $MgCl_2$, 25 mM Hepes, and 71 mM sucrose (pH 7.3, 340 mOsm) and a pipette solution containing 116 mM NMDG-Cl, 2 mM $MgSO_4$, 20 mM Hepes, 6 mM CsOH, 1 mM EGTA, 48 mM sucrose, 2 mM ATP, and 0.5 mM GTP (pH 7.2, 315 mOsm). Swelling was induced by exposure to a hypotonic (260 mOsm) bath solution that contained no added sucrose. Low NaCl solutions were prepared by isosmotic substitution of NaCl for sucrose. Oocytes were depleted of ATP by incubation for 20–30 min with 5 mM 2-deoxyglucose and 1 μM rotenone, and patch clamped with an ATP-free pipette solution containing 40 μM oligomycin, 20 μM rotenone and 5 μM iodoacetate. Metabolic inhibitors were dissolved as stock solutions in DMSO and then added to the pipette or bath saline at a final DMSO concentration of $\leq 0.01\%$.

Patch electrodes were pulled from 1.5 mm outer diameter silanized borosilicate microhaematocrit tubes; electrode resistance ranged from 2 to 4 MΩ. Currents were measured with an Axopatch 200B (Axon Instruments, Foster City, CA) patch clamp amplifier. Electrical connections to the patch clamp amplifier were made using Ag/AgCl wires and 3 M KCl/agar bridges. Data acquisition and analysis were performed using pClamp 8 software (Axon Instruments).

Measurement of HEK293 cell volume

HEK293 cells were imaged using DIC microscopy during patch clamp experiments. Cell images were recorded using a super VHS video cassette recorder (model SVO-2000; Sony Electronics Inc., San Jose, CA) and a Hamamatsu CCD camera (model C2400; Hamamatsu Photonics K.K., Hamamatsu City, Japan). The cells used for patch clamp experiments had a spherical morphology, and relative cell volume changes were therefore determined as:
$(\text{experimental CSA}/\text{control CSA})^{3/2}$, where CSA is the cell cross-sectional area measured at a single focal plane located at the point of maximum cell diameter.

Gonad immunofluorescence

Gravid adult worms were placed in 10 μl of M9 buffer (85.6 mM NaCl, 45.3 mM Na_2HPO_4, 22 mM KH_2PO_4, 1 mM $MgSO_4$, pH 7.0, 295 mOsm) on a glass slide, frozen on dry ice and freeze-cracked as described previously (Epstein & Shakes, 1995), then fixed for 10 min each in –30°C methanol and –30°C acetone. Fixed worms were rehydrated for 30 min at room temperature in 0.2% PBS-Tween, blocked with goat serum diluted to 5% with 0.2% PBS-Tween and then exposed to 1 : 50–1 : 200 dilutions of an affinity purified polyclonal antiserum raised against a fusion protein comprised of the last 132 amino acids (869–1001) of CLH-3b. Following a 60 min incubation, the slides were washed three times in 0.2% PBS-Tween and then treated for 30 min with a 1 : 1200 dilution of a Cy3-labelled goat antirabbit secondary antibody. Washed slides were mounted in Vectashield (Vector Laboratories, Burlingame, CA) and then imaged by DIC and fluorescence microscopy.

RNA interference

Double stranded RNA interference (RNA_i) was performed as described previously (Rutledge *et al.* 2001). Briefly, a

DNA template corresponding to the first 847 bp of the open reading frame of *clh-3* was obtained by PCR and sense and antisense RNA were synthesized by T7 polymerase (MEGAscript; Ambion, Austin, TX). Template DNA was digested with DNaseI and RNA was precipitated with 3 M sodium acetate and ethanol. Precipitated RNA was washed with 70% ethanol, air-dried and dissolved in water. RNA size, purity and integrity were assayed on agarose gels. dsRNA was formed by annealing sense and antisense RNA at 65°C for 30 min. Annealed dsRNA was diluted into potassium citrate buffer for injection. Worms were injected into one gonad arm with approximately 1000 000 molecules of dsRNA.

Statistical analyses

Data are presented as means ± S.E. Statistical significance was determined using Student's two-tailed *t* test for paired or unpaired means. *P*-values of ≤ 0.05 were taken to indicate statistical significance.

Results

Voltage- and time-dependent properties of CLH-3 splice variants

Figure 1 shows the amino acid sequence alignment of CLH-3a and CLH-3b. Identical regions of the two splice variants are shown by dark shading and non-identical regions are shown by light shading. Sequences outlined in a dark and a light colour denote cystathionine-β-synthase (CBS) domains and presumed intracellular N- and C-termini respectively. Note that CLH-3a and CLH-3b are identical with the exception of their N- and C-terminal cytoplasmic domains.

The functional characteristics of CLH-3 splice variants heterologously expressed in HEK293 cells were evaluated using whole-cell patch clamp recording techniques. Figure 2*A* shows current traces recorded from GFP-positive cells cotransfected with GFP and channel cDNA. Both CLH-3a and CLH-3b were constitutively active and produced robust currents that exhibited strong inward rectification and time-dependent activation at hyperpolarized test potentials. Untransfected cells ($n = 8$) or cells transfected with GFP alone ($n = 4$) exhibited no hyperpolarization-activated currents (data not shown).

The voltage-dependence of channel activation differed considerably between the two variants. Figure 2*B* shows normalized current-voltage (*I–V*) relationships for CLH-3a and CLH-3b. CLH-3b was activated at less negative test potentials resulting in a rightward shift in its *I–V* relationship compared to that of CLH-3a.

We were unable to assess the voltage dependence of channel activation for the two splice variants using tail current analysis. As reported previously for CLH-3a expressed in *Xenopus* oocytes (Schriever *et al.* 1999), we observed no tail currents for either variant due to rapid channel inactivation at positive potentials. We therefore attempted to use a negative test pulse for tail current analysis. However, the maximum apparent channel open probability of both splice variants was more negative than –170 mV (data not shown), and voltage clamping HEK293 cells beyond this voltage was difficult due to the instability of the cell membrane. Furthermore, it was not possible to estimate the minimal channel open probability for CLH-3a due to potentiation by conditioning voltages more positive than –40 mV (see below). We therefore assessed the activation characteristics of CLH-3a and CLH-3b from normalized current values fitted with a Boltzmann relation (Fig. 2*C*). The estimated half-activation potential ($V_{0.5}$) values derived from the Boltzmann fits for CLH-3a and CLH-3b were –99 ± 2 mV ($n = 11$) and –87 ± 3 mV ($n = 11$) respectively. The slope factors, *k*, for CLH-3a and CLH-3b were $10 \pm 2\ \text{mV}^{-1}$ and $18 \pm 3\ \text{mV}^{-1}$ respectively.

The activation kinetics of CLH-3a were considerably slower than those of CLH-3b. Figure 3*A* shows current traces recorded at –120 mV for the two channels. The CLH-3a current ($I_{\text{CLH-3a}}$) trace has been scaled by a factor of 1.7 and superimposed over the CLH-3b current ($I_{\text{CLH-3b}}$) trace. The time constants for activation were determined by fitting the current traces with exponential functions. $I_{\text{CLH-3a}}$ and $I_{\text{CLH-3b}}$ were well fitted by double exponentials during the first 50 ms of hyperpolarization-induced channel activation. As shown in Fig. 3*B*, the slow time constant, τ_1, was similar for both channels and voltage independent ($P > 0.5$). The fast time constant, τ_2, for CLH-3a was two- to threefold greater ($P < 0.01$) than that of CLH-3b and was voltage independent between –120 mV and –80 mV ($P > 0.17$; Fig. 3*B*). Over this same voltage range, τ_2 for CLH-3b showed a small but significant ($P < 0.01$) increase with depolarization (Fig. 3*B*).

Effect of conditioning predepolarization on CLH-3 splice variants

Schriever *et al.* (1999) reported that hyperpolarization-induced activation of CLH-3a expressed in *Xenopus* oocytes is potentiated by conditioning predepolarization. We therefore tested whether a similar voltage clamp protocol altered CLH-3a and CLH-3b activation in HEK293 cells. Transfected cells were held at 0 mV and then

voltage clamped for 1–7 s at 60 mV before stepping to –120 mV for 2 s to activate the channels. As shown in Fig. 4*A*, I_{CLH-3a} activity was potentiated by predepolarization of HEK293 cells. The extent of potentiation increased as a function of the time the cell was clamped at 60 mV (Fig. 4*A* and *B*). In contrast, I_{CLH-3b} was not potentiated by predepolarization. Instead, hyperpolarization-induced channel activity actually decreased slightly by ∼5% when cells were clamped at 60 mV for 7 s (Fig. 4*A* and *B*).

The voltage dependence of depolarization-induced potentiation is shown in Fig. 5. Transfected HEK293 cells were voltage clamped for 3 s at conditioning potentials of –20 mV to 60 mV in 20 mV increments and then stepped to –120 mV for 2 s to activate I_{CLH-3a} or I_{CLH-3b}. As shown previously (Schriever *et al.* 1999), increasing depolarization increased the extent of I_{CLH-3a} potentiation (Fig. 5*A*). In contrast, no potentiation was observed for I_{CLH-3b} at any of the test potentials examined (Fig. 5*A*).

```
CLH-3a     (1) MPSRTPLSKIEWQSLLPLPPEKSEKDATIENNEELEKIRMPAGKEYDLQPGSHLG
CLH-3b     (1) ------------------------------------------------------

CLH-3a    (56) VYKTVRGLPIDEDSKSMGIGTKILSKIEKNKTSDGLTIPLTPTTQKQSSSWCSFE
CLH-3b     (1) ----------------MGIGTKILSKIEKNKTSDGLTIPLTPTTQKQSSSWCSFE

CLH-3a   (111) SIKTFFRTVIRDWIFLALLGFIMASLSFGMDYAILNLQNGQMRLFDLVKEYHFTL
CLH-3b    (40) SIKTFFRTVIRDWIFLALLGFIMASLSFGMDYAILNLQNGQMRLFDLVKEYHFTL

CLH-3a   (166) AYLVWVGYVVGLILLSAVCAHYIAPQAIGSGIPEMKTILRGVILKEYLSVRTLLS
CLH-3b    (95) AYLVWVGYVVGLILLSAVCAHYIAPQAIGSGIPEMKTILRGVILKEYLSVRTLLS

CLH-3a   (221) KMIGLTLSLGSGLPMGKEGPFVHVASVVASQLTRLVHGSSGGIFENESRSGEMLA
CLH-3b   (150) KMIGLTLSLGSGLPMGKEGPFVHVASVVASQLTRLVHGSSGGIFENESRSGEMLA

CLH-3a   (276) AGCAVGVACTFSAPIGGVLFSIEVTSVYFAVRNYWRGFFAATCSATLFRILRMFS
CLH-3b   (205) AGCAVGVACTFSAPIGGVLFSIEVTSVYFAVRNYWRGFFAATCSATLFRILRMFS

CLH-3a   (331) VSAAVTVEAHYQTNFPPQNVFLPQELPIFALIGLVCGLAGSIFVYLHRRTVLFLR
CLH-3b   (260) VSAAVTVEAHYQTNFPPQNVFLPQELPIFALIGLVCGLAGSIFVYLHRRTVLFLR

CLH-3a   (386) RNWLAKMIFQKYWLIYPIFIATFISSLSFPLGLGKFMGGEERFSHTMKEFFVDCA
CLH-3b   (315) RNWLAKMIFQKYWLIYPIFIATFISSLSFPLGLGKFMGGEERFSHTMKEFFVDCA

CLH-3a   (441) WTAPPNDSYACPMPTSNATSSDSFDIRHWKGDNYDYSPFVTLSSFQVVYFFLAIL
CLH-3b   (370) WTAPPNDSYACPMPTSNATSSDSFDIRHWKGDNYDYSPFVTLSSFQVVYFFLAIL

CLH-3a   (496) ASTLPVPSGIFMPVFVLGAAFGRLVGEGVFSLDPYGHISGDIQFFVRPGVYAVVG
CLH-3b   (425) ASTLPVPSGIFMPVFVLGAAFGRLVGEGVFSLDPYGHISGDIQFFVRPGVYAVVG

CLH-3a   (551) AAAFCGAVTHTVSVAVIVFELTGQLCHLLPVMIAVLIANAVASYLQPSIYDSIIR
CLH-3b   (480) AAAFCGAVTHTVSVAVIVFELTGQLCHLLPVMIAVLIANAVASYLQPSIYDSIIR

CLH-3a   (606) IKNLPYLPDIPHTTSLYHQMLIEQFMISPLVYIAKDSTVGDIKRALETKTRIRAF
CLH-3b   (535) IKNLPYLPDIPHTTSLYHQMLIEQFMISPLVYIAKDSTVGDIKRALETKTRIRAF

CLH-3a   (661) PLVENMESLALVGSVSRSQLQRYVDSQIGTKARFAEATRRIKQRLEDEESERKRR
CLH-3b   (590) PLVENMESLALVGSVSRSQLQRYVDSQIGTKARFAEATRRIKQRLEDEESERKRR

CLH-3a   (716) EESKSDDTEDSLETTGAGERRAS------------------------------
CLH-3b   (645) EESKSDDTEDSLETTGAGERRASRFLIVPVAKNGPQVAKNETLTGLSEENARKIL

CLH-3a   (739) ------------------------------------------------------
CLH-3b   (700) TVEEKQALFDAASLATPKREMSGKTINPVHIESHHTIGDIFRSITHLSFGRQNFP

CLH-3a   (739) --------------RYEWEDMMLNQKLDLSQLDIDSTPFQLSEYTSLFKAHSLFS
CLH-3b   (755) KKNNHNEFDLFGEERTEWEDMMLNQKLDLSQLDIDSTPFQLSEYTSLFKAHSLFS

CLH-3a   (780) LLGLNRAYVTKKGQLIGVVALKEVCFLISRKK----------------------
CLH-3b   (810) LLGLNRAYVTKKGQLIGVVALKELRLAIEYLQSGKVPTPGMSIFNEPPTEQSIYE

CLH-3a   (812) ------------------------------------------------------
CLH-3b   (865) KSARLESGRATGDAQNAAFVTDNGEDDAQNDYIQPPLEVVRRGALTPNRMSELTR

CLH-3a   (812) ------------------------------------------------------
CLH-3b   (920) LENVRTTPESPHFEVSSPSTSSSCVSIDFSPLDAANSENGSVGGLVLNVPSLPTR

CLH-3a   (812) --------------------------
CLH-3b   (975) ARSANELTRQNTHVQINLPDDVHDEKF
```

Figure 1. Sequence alignment of CLH-3a and CLH-3b
Regions of identity are shown by dark shading and non-identical regions are shown by light shading. Regions outlined in a light colour are the presumed intracellular N- and C-termini. Cystathionine-β-synthase (CBS) domains are outlined in black. Alignment was performed using Vector NTI software (InforMax, Bethesda, MD).

Figure 5*B* summarizes the effect of conditioning predepolarization on peak I_{CLH-3a} and I_{CLH-3b} amplitude measured between 170 ms and 270 ms after the onset of the –120 mV test pulse. This time domain was chosen because it bracketed the maximal amplitude of I_{CLH-3a} measured after pulses to depolarized conditioning potentials (Fig. 5*A*). Peak current values measured after each conditioning potential were normalized to that measured following a conditioning potential of –20 mV. The amplitude of I_{CLH-3a} increased steeply with the strength of the conditioning potential. For example, I_{CLH-3a} amplitude measured following a 60 mV conditioning potential was 1.96 ± 0.08-fold ($n = 17$) greater than that measured after a –20 mV conditioning potential. In contrast, I_{CLH-3b} amplitude measured following a conditioning potential of 60 mV increased only slightly by 1.08 ± 0.03-fold ($n = 8$) over that measured after the –20 mV conditioning potential. This increase was significantly ($P < 0.0001$) less than that observed for I_{CLH-3a}.

We also found that conditioning depolarization induced inactivation of I_{CLH-3a} (Fig. 5*A*). Figure 5*C* summarizes the voltage dependence of inactivation for the two splice variants. The data are presented as fractional current, where the mean pseudo steady-state current amplitude (I_{SS}) measured during the last 20 ms of the –120 mV test pulse is divided by the peak current amplitude (I_{peak}). I_{CLH-3a} inactivation was rarely observed following a conditioning potential of –20 mV, but became evident with stronger depolarizing prepotentials (Fig. 5*C*). For example, predepolarization to 60 mV caused I_{CLH-3a} to inactivate by 21 ± 2% over the 2 s, –120 mV test potential. In contrast, conditioning predepolarization failed to induce I_{CLH-3b} inactivation (Fig. 5*A* and *C*).

The time constants that describe I_{CLH-3a} activation and inactivation as a function of conditioning potential are shown in Fig. 6. Activation time constants were derived by fitting a double exponential to the first 50 ms of hyperpolarization-induced channel activation. The inactivation process was well described by fitting a single exponential to the entire time course of inactivation. The conditioning potential had no significant ($P > 0.12$) effect on any of the time constants.

Sensitivity of CLH-3 splice variants to extracellular Cl^- and H^+

Voltage-dependent gating of some ClC channels is coupled to extracellular Cl^-, and reductions in Cl^- concentration decrease channel open probability (reviewed in Jentsch *et al.* 2002). We therefore characterized the effect of external Cl^- concentration on I_{CLH-3a} and I_{CLH-3b}. Whole-cell currents were recorded under control conditions (92 mM Cl^-) and at 30 s after switching to a low Cl^-

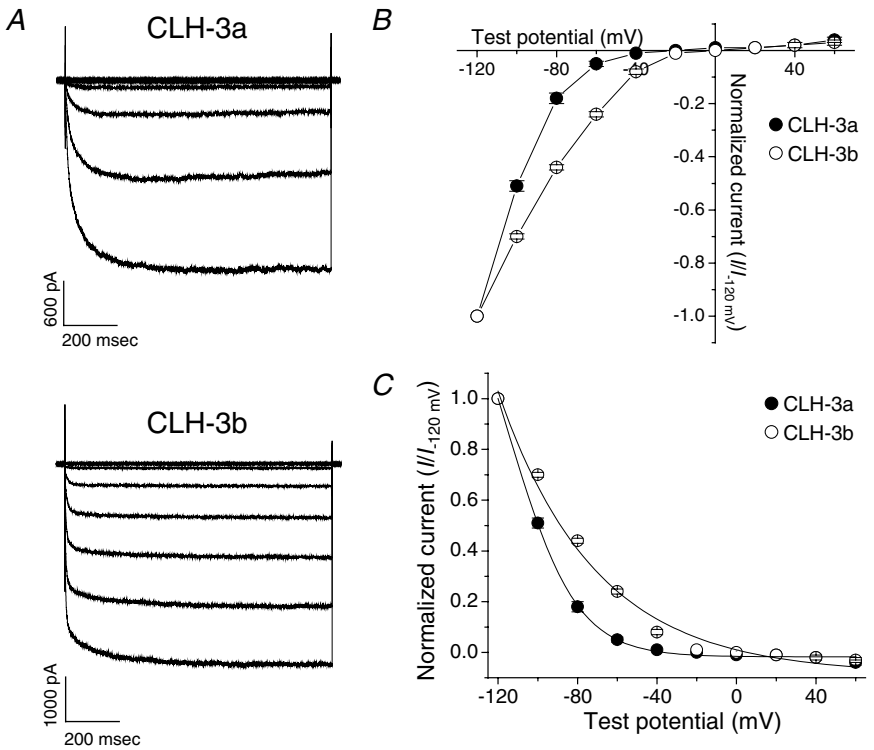

Figure 2. Voltage-dependent properties of CLH-3a and CLH-3b
A, representative current traces from HEK293 cells cotransfected with GFP and CLH-3a or CLH-3b cDNAs. Whole-cell Cl^- currents were evoked by stepping membrane voltage for 1 s between –120 mV and +60 mV in 20 mV increments from a holding potential of 0 mV. Each test pulse was followed by a 1 s interval at 0 mV. *B*, normalized *I–V* relationships for CLH-3a and CLH-3b. Steady state current amplitude recorded at each test potential was normalized to that measured at –120 mV. Values are means ± S.E. ($n = 11$). *C*, Boltzmann fits of normalized *I–V* relationships for I_{CLH-3a} and I_{CLH-3b}. Fits were performed using the equation $I(V_m) = ([A_1 - A_2]/[1 + e^{(Vm-V0.5)/k}]) + A_2$, where $V_{0.5}$ is the half-activation potential and k is the slope factor.

(12 mM) bath solution. In the absence of regulatory effects, reductions in extracellular Cl^- concentration are expected to increase inward current due to an increase in the outward driving force on the ion. Figure 7*A* and *B* show normalized *I–V* relationships for CLH-3a and CLH-3b recorded in control and low Cl^- bath solutions. Reduction of the bath Cl^- significantly ($P < 0.01$) inhibited I_{CLH-3a} at test potentials of –80 mV to –120 mV (Fig. 7*A*), but had no effect ($P > 0.3$) on I_{CLH-3b} (Fig. 7*B*). As summarized in Fig. 7*C*, mean I_{CLH-3a} amplitude at –100 mV was 1.8-fold greater in the presence of 92 mM Cl^- *versus* 12 mM Cl^-. This effect was due specifically to reduction of the bath Cl^- as replacement of NaCl with NMDG-Cl had no significant ($P = 0.98$) effect on I_{CLH-3a} amplitude ($n = 3$; data not shown).

Several ClC channels are activated by acidification of the extracellular solution (reviewed in Jentsch *et al.* 2002). It has been suggested that external H^+ and Cl^- may act at a common site to increase channel open probability (Rychkov *et al.* 1996; Dutzler *et al.* 2003). The difference in sensitivity of CLH-3a and CLH-3b to

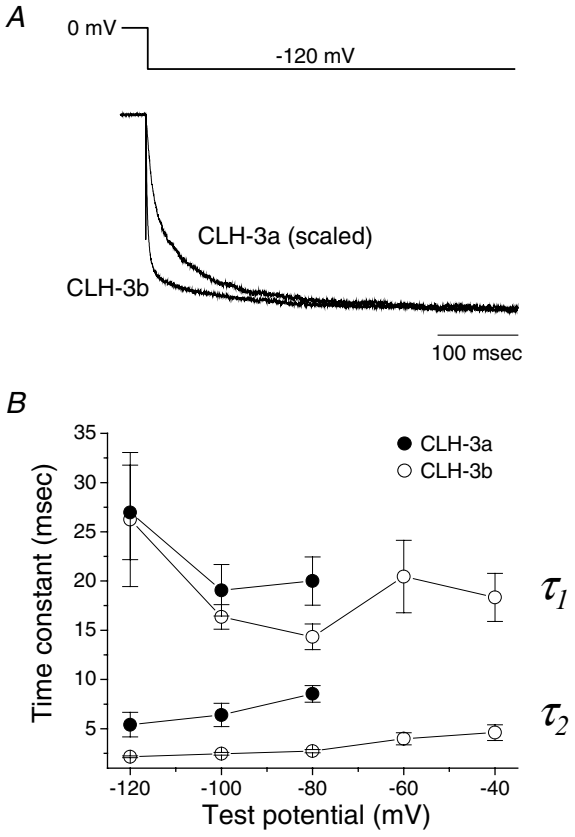

Figure 3. Kinetics of CLH-3a and CLH-3b activation
A, representative current traces showing activation kinetics of CLH-3 splice variants at –120 mV. The I_{CLH-3a} trace was scaled by a factor of 1.7 and superimposed over the I_{CLH-3b} trace for comparison of activation time courses. *B*, slow (τ_1) and fast (τ_2) time constants for CLH-3a and CLH-3b. Time constants were derived by fitting the first 50 ms of hyperpolarization-induced current activation with a double exponential function. Activation of CLH-3a was nominal at –60 mV (Fig. 2*B*) and time constants could be accurately derived only at more hyperpolarized voltages. Values are means ± S.E. (n = 8–9).

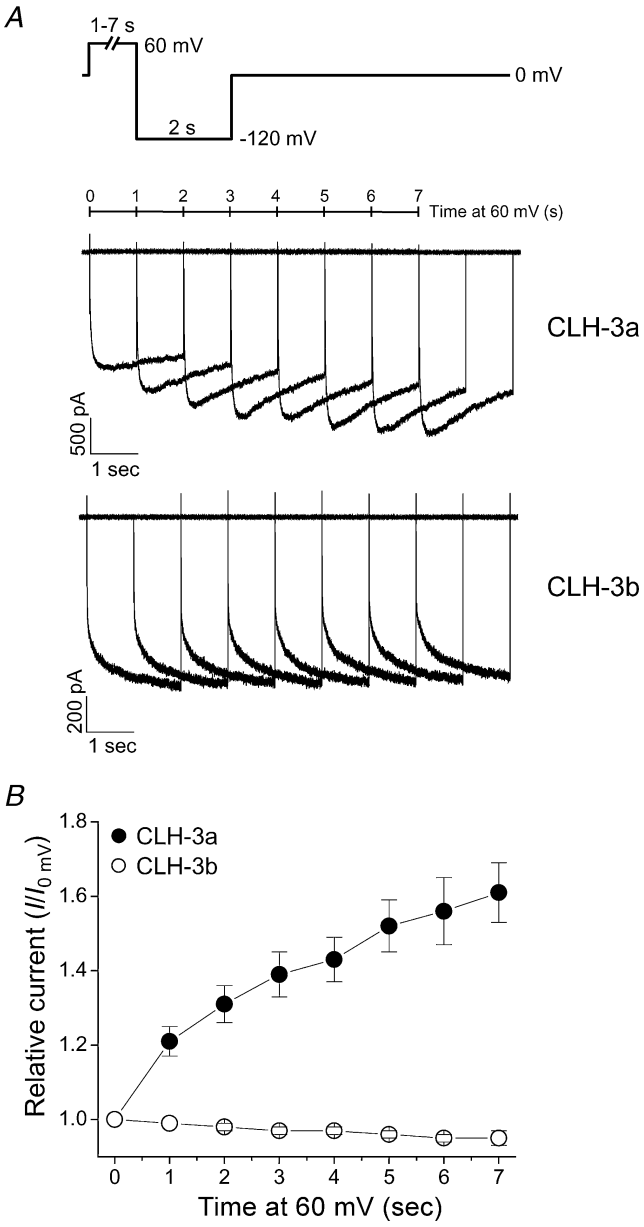

Figure 4. Time-dependent effects of predepolarization on hyperpolarization-induced activation of CLH-3a and CLH-3b
A, transfected HEK293 cells were voltage clamped for 1–7 s at 60 mV from a holding potential of 0 mV and then stepped to –120 mV for 2 s to activate the expressed channels. *B*, time dependency of predepolarization on peak I_{CLH-3a} and I_{CLH-3b} amplitude measured between 170 ms and 270 ms after the onset of the –120 mV test pulse. Currents are plotted relative to those measured from the holding potential of 0 mV (i.e. I_0 mV). Values are means ± S.E. ($n = 6$).

Cl^- suggested that the two variants would also exhibit different sensitivities to extracellular H^+. To test this idea, we measured I_{CLH-3a} and I_{CLH-3b} in control pH 7.4 saline and at 30 s after changing the bath pH to 5.9, 6.5, or 8.1. Representative *I–V* relationships at different extracellular pH values for I_{CLH-3a} and I_{CLH-3b} are shown in Fig. 8*A* and *B*. CLH-3a was considerably more sensitive to changes in extracellular H^+ concentration than CLH-3b. Figure 8*C* shows that I_{CLH-3a} amplitude increased ~13-fold as extracellular H^+ concentration was increased from pH 8.1 to pH 5.9. In contrast, CLH-3b activity increased by only ~2.2-fold over this pH range (Fig. 8*C*).

We also found that the voltage dependence of the acidification-induced activation differed for the two variants. Figure 8*D* shows a plot of the pH 6.5-induced increase in current amplitude as a function of test potential. Activation of I_{CLH-3a} by acidification was strongly potentiated by depolarization. At –60 mV, the mean ± s.e. acidification-induced increase in current amplitude was 2.36 ± 0.4-fold ($n = 12$) greater than that observed at –120 mV. In contrast, depolarization had relatively little effect on I_{CLH-3b} (Fig. 8*D*). The mean ± s.e. relative acidification-induced increase of I_{CLH-3b} at –60 mV *versus* –120 mV was 1.25 ± 0.03 ($n = 8$). This value is significantly ($P < 0.03$) less than that observed for I_{CLH-3a}.

Regulation of CLH-3 splice variants by cell swelling

Hypotonicity-induced cell swelling activates native CLH-3 expressed in *C. elegans* oocytes (Fig. 9 and Rutledge

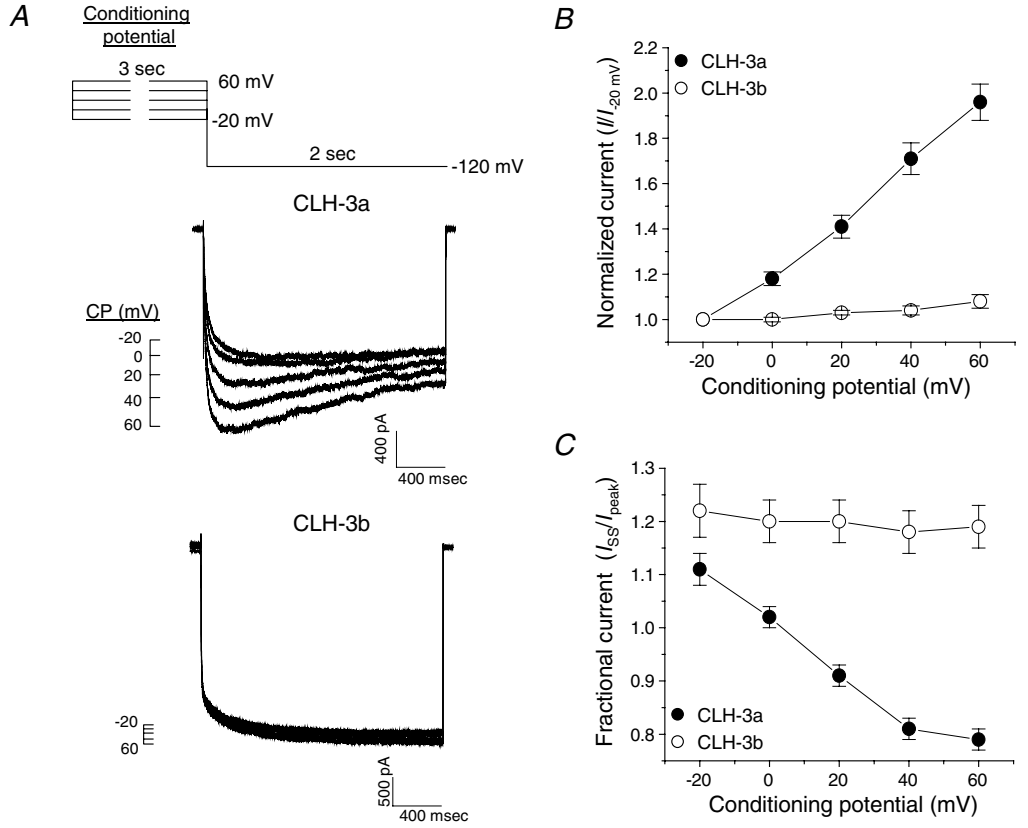

Figure 5. Voltage-dependent effects of predepolarization on hyperpolarization-induced activation and inactivation CLH-3a and CLH-3b

A, representative current traces at –120 mV from CLH-3a- and CLH-3b-transfected HEK293 cells. Cells were voltage clamped for 3 s at condition potentials (CP) from –20 mV to 60 mV and then stepped to –120 mV for 2 s to activate the expressed channels. *B*, effect of conditioning potential on hyperpolarization-induced activation of I_{CLH-3a} and I_{CLH-3b}. Peak current amplitude was measured between 170 ms and 270 ms after stepping to –120 mV. Current values were normalized to that measured following a conditioning pulse of –20 mV (i.e. I_{-20} mV). Values are means ± s.e. ($n = 8$–17). *C*, effect of conditioning potential on inactivation of I_{CLH-3a} and I_{CLH-3b}. Mean normalized pseudo-steady-state current (I_{SS}) was measured over the last 20 ms of the –120 mV test pulse and normalized to peak current (I_{peak}) amplitude. Values are means ± s.e. ($n = 8$–17).

et al. 2001). To determine whether CLH-3 splice variants exhibit differences in their volume sensitivity, we measured CLH-3a and CLH-3b current amplitude in transfected HEK293 cells 1 min after reducing bath osmolality from 295 mOsm to 225 mOsm. Cell swelling during this time period is insufficient to activate the ubiquitous outwardly rectifying Cl^- current $I_{Cl,swell}$ (Rutledge *et al.* 2002).

Mean ± S.E. relative cell volume 1 min after exposure of patch clamped HEK293 to hypotonicity was 1.6 ± 0.1 ($n = 8$); no significant ($P > 0.5$) difference was observed in the extent of swelling in CLH-3a- *versus* CLH-3b-transfected cells. Cell swelling activated I_{CLH-3a} and I_{CLH-3b} by ~20%. Mean ± S.E. relative whole-cell currents in hypotonically swollen CLH-3a- and CLH-3b-transfected cells were 1.19 ± 0.04 ($n = 4$) and 1.23 ± 0.06 ($n = 4$) respectively. These values were not significantly ($P > 0.5$) different.

Biophysical characteristics of the native oocyte Cl^- current

The existence of two CLH-3 splice variants with unique structural and biophysical properties suggests that the channels perform distinct physiological roles. To begin addressing this important issue, we carried out a detailed biophysical characterization of the native oocyte Cl^- current.

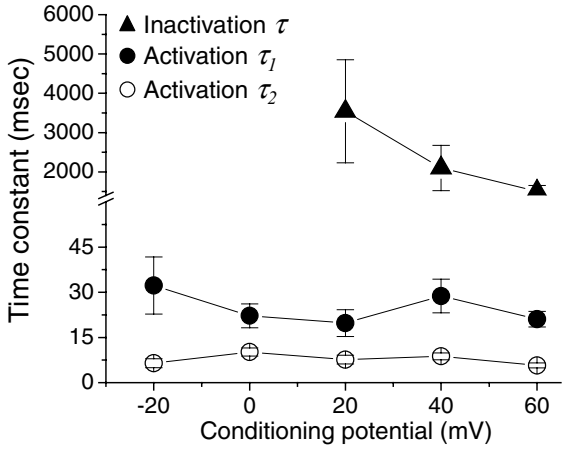

Figure 6. Effects of predepolarization on time constants of activation and inactivation of CLH-3a
CLH-3a-expressing HEK293 cells were voltage clamped for 3 s at condition potentials from –20 mV to 60 mV and then stepped to –120 mV for 2 s to activate the channel. Slow (τ_1) and fast (τ_2) activation time constants were derived by fitting the first 50 ms of hyperpolarization-induced current activation with a double exponential function. The inactivation time constant (τ) was derived by fitting the entire time course of current inactivation with a single exponential function. Values are means ± S.E. (n = 9).

Figure 9*A* shows whole-cell currents in a non-maturing wild-type oocyte under basal conditions and after maximal current activation induced by hypotonic swelling for 9 min. Also shown are whole-cell currents in an oocyte isolated from a *clh-3(ok763)* mutant worm. The *clh-3(ok763)* oocyte was swollen for 10 min. *I–V* relationships for the three whole-cell currents are shown in Fig. 9*B*. No inwardly rectifying Cl^- current was observed in

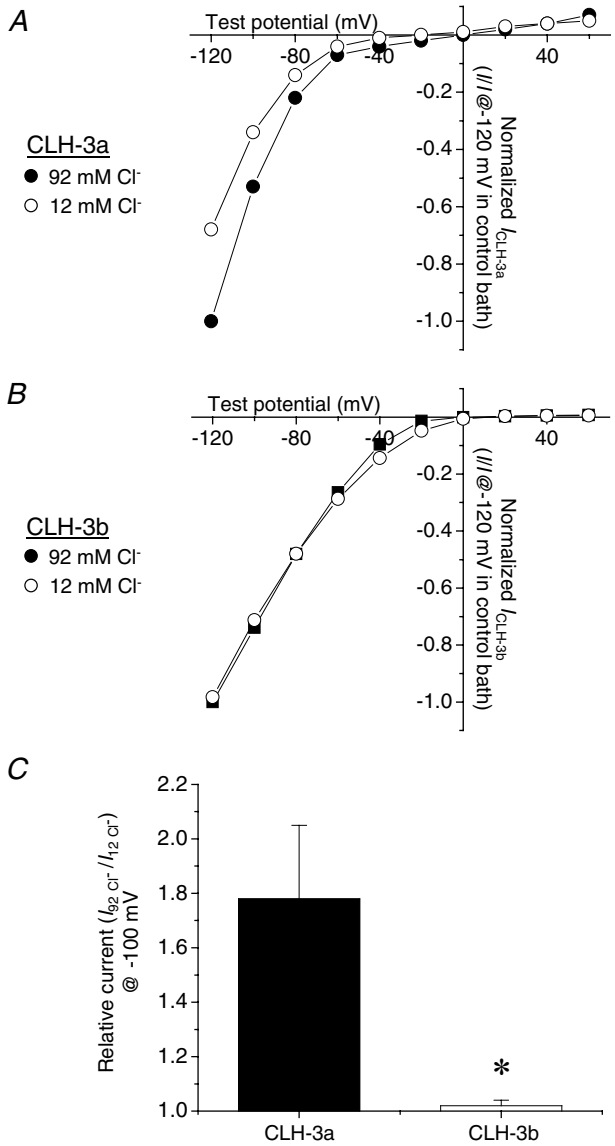

Figure 7. Effects of extracellular Cl^- on CLH-3a and CLH-3b
A and *B*, representative *I–V* relationships for I_{CLH-3a} and I_{CLH-3b} respectively, recorded in 92 mM Cl^- control bath solution and at 30 s after switching to a 12 mM Cl^- bath solution. Current values measured at each test potential were normalized to that measured at –120 mV in 92 mM Cl^- bath solution. *C*, relative amplitude for I_{CLH-3a} and I_{CLH-3b} measured at –100 mV in 92 mM Cl^- bath solution *versus* 12 mM Cl^-. Values are means ± S.E. ($n = 5$–7). $^*P < 0.004$ compared to CLH-3a.

clh-3(ok763) oocytes under basal conditions or after prolonged (8–15 min) swelling ($n = 7$). The *ok763* allele is an ∼1500 bp deletion in the *clh-3* gene. The absence of hyperpolarization-induced Cl^- currents in *clh-3(ok763)* oocytes demonstrates that both basal and swelling-activated inwardly rectifying Cl^- channels are encoded by *clh-3*, a finding that is consistent with our previous RNA_i studies (Rutledge *et al.* 2001).

We measured the time constants of activation of native I_{CLH-3}at various test voltages. To facilitate comparison of the native current with heterologously expressed CLH-3a and CLH-3b, we measured slow (τ_1) and fast (τ_2) time constants by fitting a double exponential to the first 50 ms of hyperpolarization-induced current activation. Figure 9*C* shows the time constants plotted as a function voltage. Both the τ_1 and τ_2 of native I_{CLH-3} were similar to those of I_{CLH-3b} and showed similar voltage dependencies. The constant τ_1 was voltage insensitive ($P > 0.5$) and τ_2 showed a small but significant ($P < 0.002$) increase with depolarization ($n = 9$).

Figure 10*A* shows the voltage dependence of predepolarization on native I_{CLH-3} when activated by oocyte swelling. The oocyte was voltage clamped for 3 s at conditioning potentials of –20 mV to 60 mV and then stepped to −120 mV for 2 s. No potentiation of the current was observed at any of the voltages tested.

In addition to native I_{CLH-3} activated by oocyte swelling, we quantified the effects of predepolarization on basal I_{CLH-3} activity, on I_{CLH-3} activated by oocyte meiotic maturation, and on I_{CLH-3} activated by intracellular ATP depletion, which activates the current by inducing net protein dephosphorylation (Rutledge *et al.* 2002). Figure 10*B* shows the relative I_{CLH-3} amplitude at –120 mV following a 3 s predepolarization to either 60 mV or –20 mV. Predepolarization had no significant ($P > 0.14$) effect on native I_{CLH-3} under any of the conditions tested.

To assess whether prolonged depolarization would potentiate native I_{CLH-3}, we measured the effect of voltage clamping swollen oocytes to 60 mV for 1–7 s. As shown

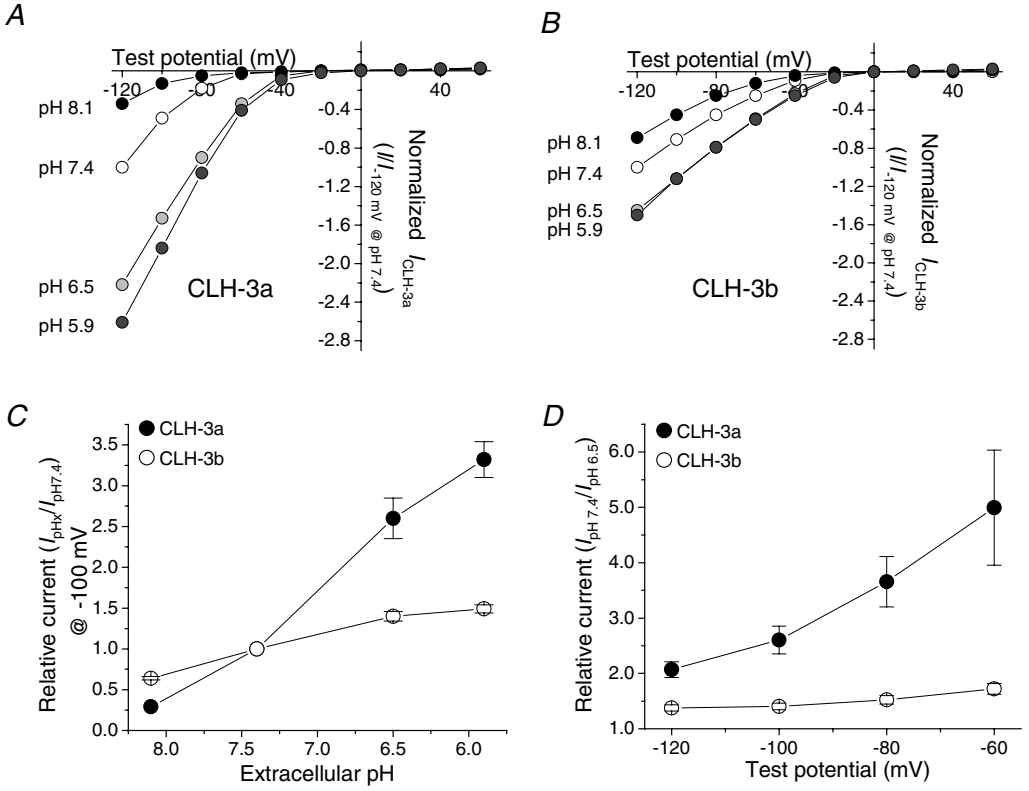

Figure 8. Effect of extracellular acidification on CLH-3a and CLH-3b
A and *B*, representative *I–V* relationships for I_{CLH-3a} and I_{CLH-3b} respectively, recorded in pH 7.4 control bath and at 30 s after switching to pH 5.9, pH 6.5, or pH 8.1 bath solutions. *C*, effects of changes in extracellular pH on I_{CLH-3a} and I_{CLH-3b} measured at –100 mV. Values are means ± S.E. (n = 4–12). *D*, voltage dependence of the pH 6.5-induced activation of I_{CLH-3a} and I_{CLH-3b}. Values are means ± S.E. (n = 8–12).

in Fig. 10*C* and *D*, native I_{CLH-3} was not potentiated by depolarization. Instead, current amplitude declined slightly as a function of the time oocytes were depolarized. Following a 7 s predepolarization to 60 mV, native I_{CLH-3} amplitude was reduced by ∼7% (Fig. 10*D*). This small decrease in current is similar to that observed for I_{CLH-3b} in HEK293 cells (Fig. 4*B*).

We also characterized the effects of extracellular Cl^- and pH on native I_{CLH-3}. Whole-cell current was measured in the presence of control saline containing 124 mM Cl^- and at 30 s after switching to a 16 mM Cl^- bath solution. This represents an 87% reduction in extracellular Cl^-, which is identical to the change in bath Cl^- used to evaluate the heterologously expressed CLH-3 splice variants. Figure 11*A* shows the mean ± S.E. *I–V* relationships for native I_{CLH-3} activated by swelling in 124 mM and 16 mM Cl^- bath solutions. Reduction of the bath Cl^- had no significant ($P > 0.1$) effect on native I_{CLH-3} at test potentials of –100 mV to –60 mV. However, at −40 mV, reduction of the bath Cl^- caused a small but significant ($P < 0.01$) increase in native I_{CLH-3} amplitude. The lack of change in current amplitude at –100 mV during reduction of the bath Cl^- is identical to that observed for I_{CLH-3b} (Fig. 7*C*).

The effect of extracellular acidification on native I_{CLH-3} measured at –100 mV is shown in Fig. 11*B*. The data have been plotted on the same scale used in Fig. 8*C* for comparison with I_{CLH-3a} and I_{CLH-3b}. Swelling-activated native I_{CLH-3} was measured in pH 7.3 bath solution and at 30 s after changing the bath pH to 5.9, 6.5, or 8.1. Increasing the bath H^+ concentration from pH 8.1 to pH 5.9 increased the native I_{CLH-3} amplitude ∼2-fold, similar to that observed for I_{CLH-3b} (Fig. 8*C*).

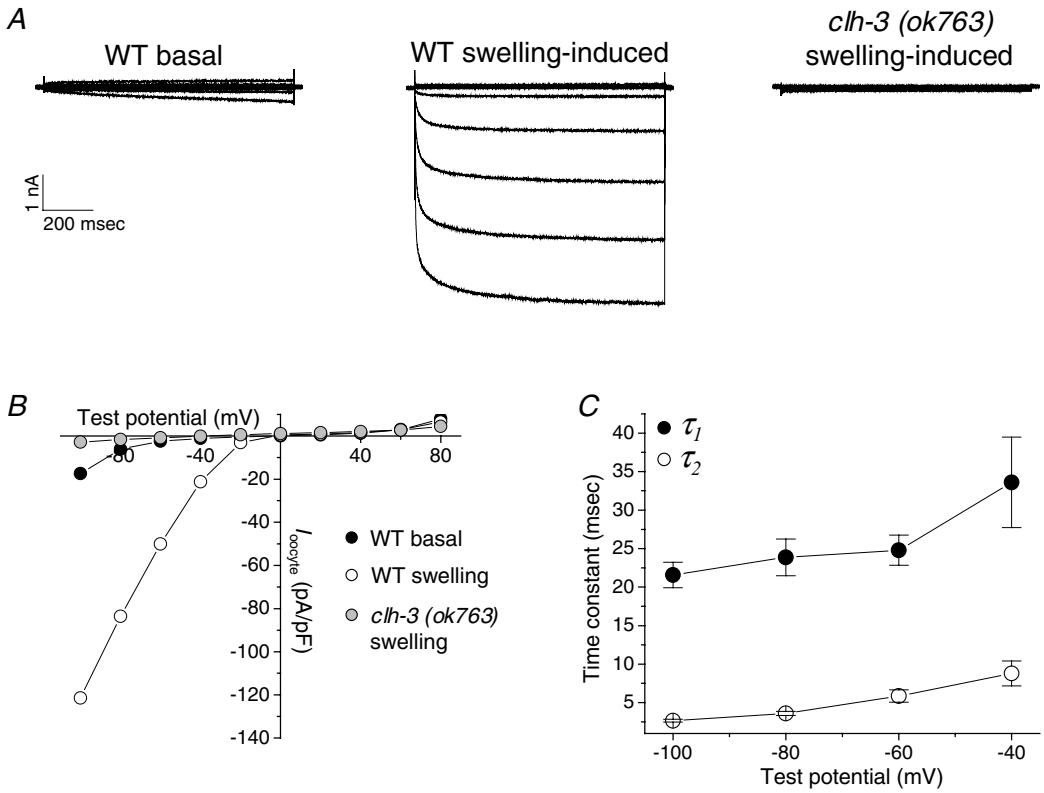

Figure 9. Activation kinetics of native I_{CLH-3}

A, representative whole-cell Cl^- current traces under basal conditions and after maximal activation by swelling in an oocyte isolated from a wild-type (WT) worm and in an oocyte isolated from a *clh-3(ok763)* mutant worm. The *clh-3(ok763)* oocyte was swollen for 10 min. Currents were evoked by stepping membrane voltage for 1 s between –100 mV and +60 mV in 20 mV increments from a holding potential of 0 mV. Each test pulse was followed by a 1 s interval at 0 mV. The corresponding *I–V* relationships for these currents are shown in *B*. *C*, time constants for hyperpolarization-induced activation of native I_{CLH-3a} in swollen oocytes. Values are means ± S.E. ($n = 4$–8).

As shown in Fig. 11*C*, the voltage dependence of the acidification effect was weak and similar to that of I_{CLH-3b} (Fig. 8*D*). At −40 mV, the mean ± s.e. acidification-induced increase in current amplitude was 1.22 ± 0.05-fold (n = 7) greater than that observed at –100 mV. The mean ± s.e. relative acidification-induced increase of I_{CLH-3b} at −40 mV *versus* −100 mV was 1.52 ± 0.09-fold (n = 8).

Immunolocalization of CLH-3b in *C. elegans* oocytes

The *C. elegans* adult hermaphrodite gonad consists of two U-shaped arms connected to a common uterus. The distal gonad contains germline nuclei embedded in a syncitial cytoplasm. In the loop region of the gonad, a plasma membrane forms around these nuclei in a process termed 'cellularization'. Newly formed oocytes develop in the proximal region of the gonad and accumulate in a single row of graded developmental stages. The most differentiated oocyte is positioned adjacent to the spermatheca where it undergoes meiotic maturation and is then ovulated into the spermatheca and fertilized (reviewed by Hubbard & Greenstein, 2000).

The native oocyte Cl^- current has biophysical properties virtually indistinguishable from those of heterologously expressed CLH-3b. To determine whether CLH-3b is translationally expressed in oocytes, we generated a polyclonal antiserum against the last 132 amino acids

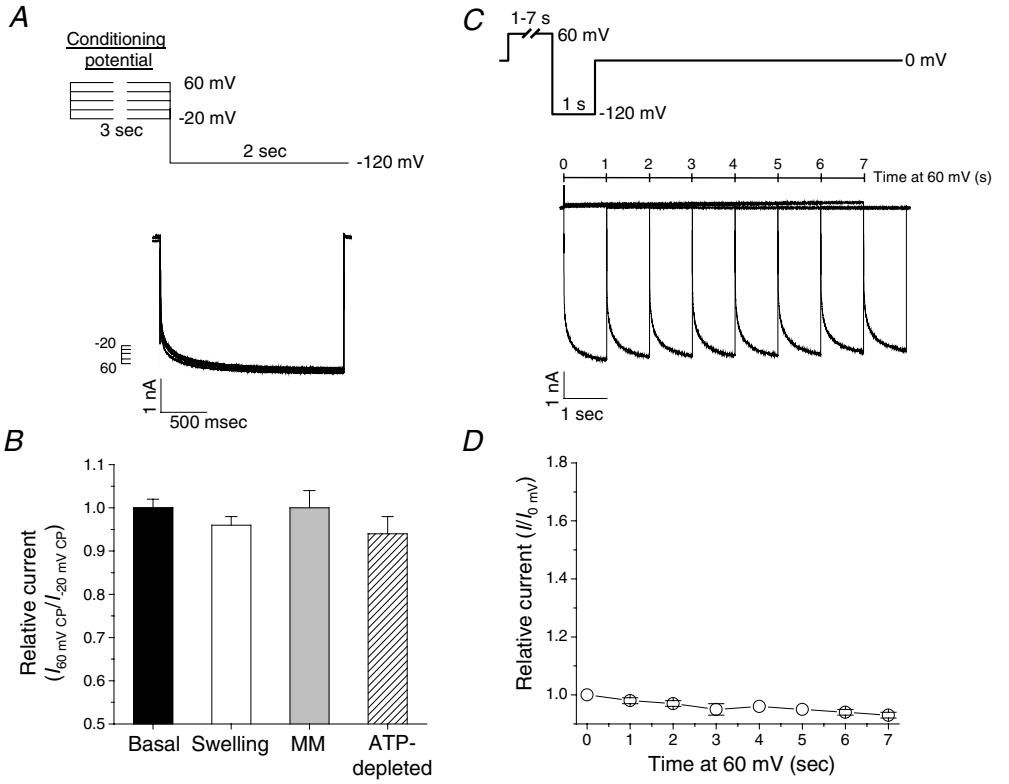

Figure 10. Voltage- and time-dependent effects of predepolarization on hyperpolarization-induced activation of native I_{CLH-3}

A, representative whole-cell current traces at −120 mV in a swollen wild-type oocyte. The oocyte was voltage clamped for 3 s at conditioning potentials (CP) from –20 mV to 60 mV and then stepped to −120 mV for 1 s to activate native I_{CLH-3}. *B*, effect of predepolarization on native I_{CLH-3}at –120 mV under basal conditions and after current activation by oocyte swelling, oocyte meiotic maturation (MM) or ATP depletion. Peak current amplitudes were quantified between 170 ms and 270 ms after the onset of the –120 mV test pulse following a predepolarization of –20 mV or 60 mV. Values are means ± s.e. (n = 3–12). *C*, time-dependence of predepolarization on native I_{CLH-3} in a swollen oocyte. Oocytes were voltage clamped for 1–7 s at 60 mV from a holding potential of 0 mV and then stepped to –120 mV for 1 s to activate native I_{CLH-3}. *D*, Mean I_{CLH-3} amplitude at –120 mV in swollen oocytes plotted as a function of the time they were clamped at a conditioning potential of 60 mV. Currents are plotted relative to those measured from the holding potential of 0 mV (i.e. I_0 mV). Data are shown on the same *Y*-axis scale as Fig. 4*B* to facilitate comparison with heterologously expressed splice variants. Values are means ± s.e. (n = 3).

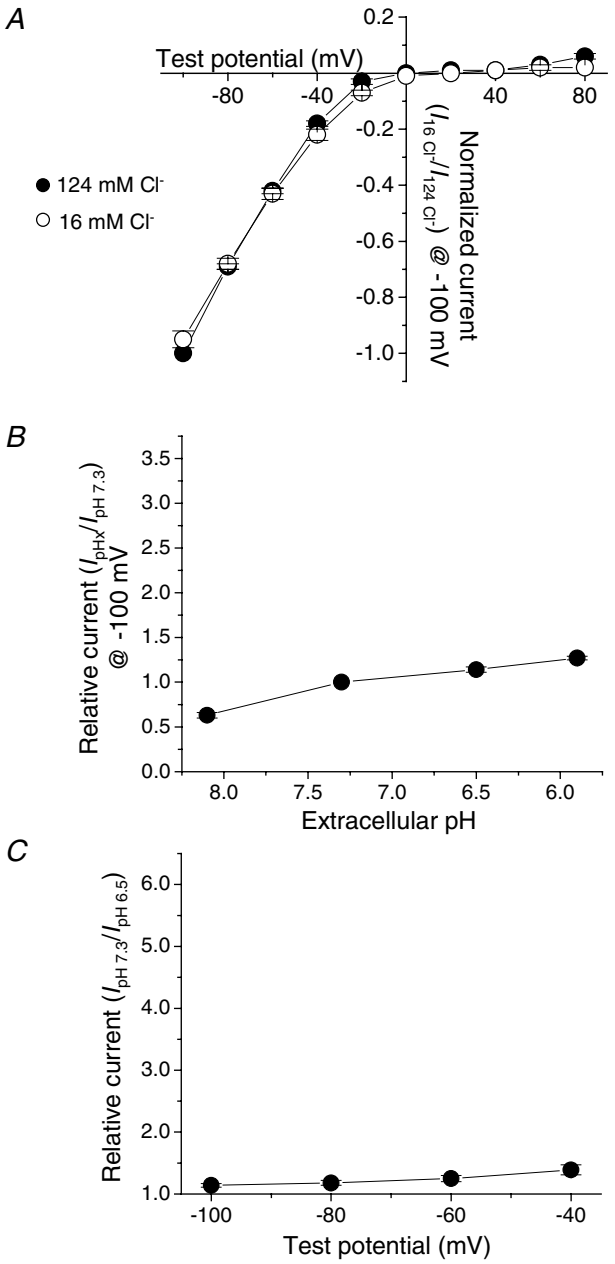

Figure 11. Effect of extracellular Cl^- and pH on native I_{CLH-3}
A, *I–V* relationships of swelling-activated native I_{CLH-3} in 124 mM Cl^- control saline and at 30 s after switching to a 16 mM Cl^- bath solution. Values are means ± S.E. ($n = 7$). *B*, relative change in native I_{CLH-3}current amplitude after switching from a pH 7.3 bath solution to pH 5.9, pH 6.5, or pH 8.1 bath solutions. The data have been plotted on the same scale as Fig. 8*C* for comparison with I_{CLH-3a} and I_{CLH-3b}. Values are means ± S.E. ($n = 4$–7). *C*, voltage dependence of native I_{CLH-3} activation by bath acidification to pH 6.5. Relative current values are plotted on the same Y-axis scale used in Fig. 8*D* for comparison with heterologously expressed splice variants. Values are means ± S.E. ($n = 7$).

of the channel protein. Isolated gonads were fixed and immunostained using this antiserum and a Cy3-labelled secondary antibody. As shown in Fig. 12*A* and *B*, CLH-3b was detected in the plasma membrane at all stages of oocyte development, including newly formed oocytes in the loop region of the gonad. A faint cytoplasmic and occasionally a nuclear background staining were observed when gonads were reacted with the preimmune serum or with antiserum that had been previously competed with an 85-fold molar excess of the CLH-3b fusion protein (data not shown). Gonads in which *CLH-3* expression was disrupted by RNA_i showed faint cytoplasmic and nuclear staining (Fig. 12*C*) similar to that observed with the preimmune serum or the CLH-3b fusion protein-competed antiserum. These results demonstrate that CLH-3b is expressed in the *C. elegans* oocyte beginning at very early stages of oocyte development when the plasma membrane is first formed around germline nuclei.

Discussion

Effects of splice variation on CLH-3 gating and regulation

Alternative splicing increases the functional diversity of numerous channel types (Fettiplace & Fuchs, 1999; Lipscombe *et al.* 2002). However, almost nothing is known about the role of alternative splicing in ClC function and regulation. We have demonstrated in this work that splice variation of the predicted intracellular N- and C-termini of CLH-3 causes significant changes in channel biophysical properties.

Both CLH-3a and CLH-3b are activated by cell swelling and membrane hyperpolarization. However, the splice variants exhibit significant differences in activation kinetics and voltage sensitivity. Hyperpolarization-induced activation of CLH-3b is approximately threefold faster than that of CLH-3a (Fig. 3*A* and *B*). In addition, CLH-3b is active at physiologically relevant membrane voltages (i.e. −40 mV to −60 mV) whereas CLH-3a requires much stronger hyperpolarization for activation (Fig. 2*B* and *C*).

A particularly striking difference between CLH-3a and CLH-3b is their sensitivity to conditioning voltages. As reported previously (Schriever *et al.* 1999), we found that predepolarization activated CLH-3a and induced slow inactivation of the current at hyperpolarized potentials (Figs 4 and 5). Schriever *et al.* (1999) showed that increased extracellular Cl^- activates CLH-3a during the depolarizing prepulse and that the degree

of predepolarization-induced activation is dependent on the concentration of the bath Cl^-. They further demonstrated that activation of CLH-3a by depolarizing prepulses and increased extracellular Cl^- had similar time courses. The effect of predepolarization on CLH-3a was attributed to a slow gating process that is regulated by both membrane potential and extracellular Cl^- (Schriever *et al.* 1999).

It is conceivable that membrane potential *per se* does not regulate the putative CLH-3a slow gate. Instead, prolonged depolarization may raise local Cl^- concentration near the proposed Cl^- binding site that is thought to regulate ClC gating (Chen & Miller, 1996; Dutzler *et al.* 2003). In this regard, it is interesting to note that predepolarization has almost no effect on the amplitude of I_{CLH-3b} (Figs 4 and 5) and the channel is relatively insensitive to changes in the bath Cl^- concentration (Fig. 7*B*-*C*). The insensitivity of CLH-3b to depolarizing prepulses may be due to a relative insensitivity of the gating mechanism to extracellular Cl^-.

We found that of the two splice variants, CLH-3a is activated to a much greater degree by extracellular acidification (Fig. 8). The effect of extracellular pH on ClC channel activity has been attributed either to a direct effect of extracellular H^+ on the activation gate (Rychkov *et al.* 1996; Rychkov *et al.* 1997; Dutzler *et al.* 2003), or to changes in surface charge resulting from H^+ binding to anionic sites in or near the channel pore (Arreola *et al.*

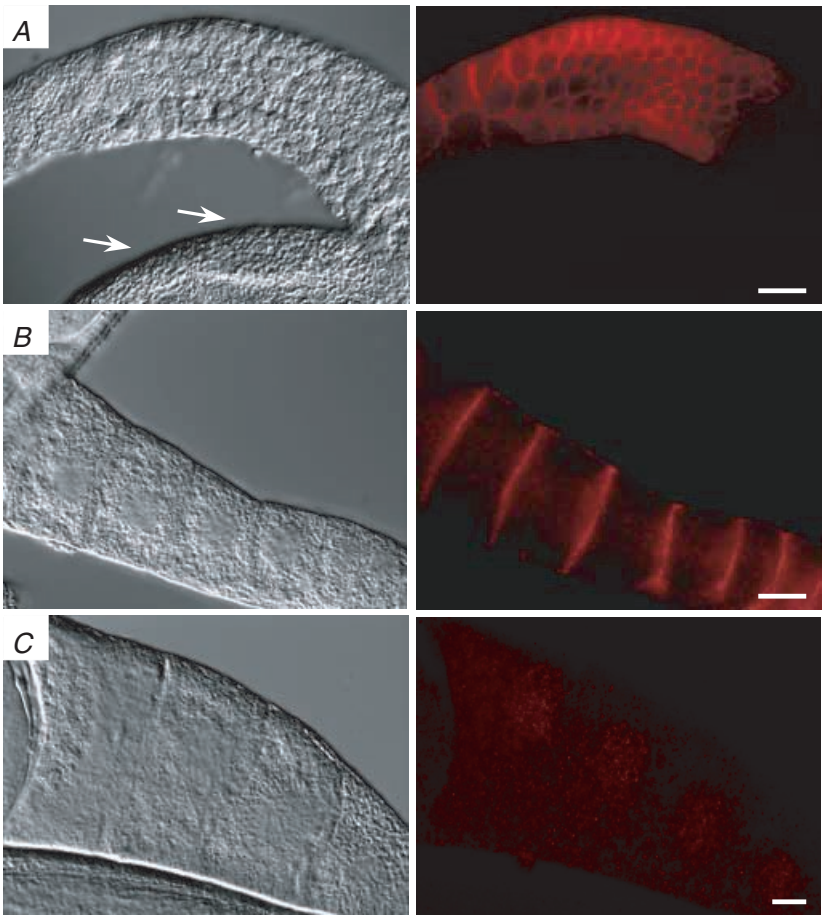

Figure 12. Immunolocalization of CLH-3b in the *C. elegans* gonad
Differential interference contrast (left panels) and fluorescence (right panels) micrographs of isolated *C. elegans* gonads. *A*, section of distal (arrows) and beginning of proximal gonad. CLH-3b immunostaining is first detected in the loop region of the gonad where germ cell nuclei are cellularized. *B*, section of proximal gonad containing single oocytes. *C*, section of proximal gonad isolated from a worm injected with *clh-3* dsRNA. Faint background staining is similar to that observed in gonads immunoreacted with preimmune serum and in gonads in which CLH-3b antiserum was competed with CLH-3b fusion protein (data not shown). Fluorescence image exposure time is 300 ms in *A*, 200 ms in *B* and 1 s in *C*. Antiserum was diluted 1 : 50 (*A*) or 1 : 200 (*B* and *C*). Scale bars are 20 μm.

2002; Ferroni *et al.* 2000; Jordt & Jentsch, 1997). One possible explanation for the difference in pH sensitivity of CLH-3a and CLH-3b is that splice variation may alter the H^+ affinities and/or accessibility of titratable residues that regulate channel activation. While we cannot define at present the mechanism by which acidification activates CLH-3, the differences in the effects of predepolarization, extracellular Cl^- concentration and pH on the splice variants suggest that all three may act on a single gating mechanism that differs between the two channels.

How might alternative splicing of presumed intracellular N- and C-termini affect the sensitivity of CLH-3 to predepolarization and extracellular ions? Dutzler *et al.* (2002,2003) recently identified in the high-resolution crystal structures of bacterial ClC channels, a highly conserved glutamate residue in the outer channel pore that may serve as a Cl^--and H^+-dependent activation gate. In the closed state, the glutamate carboxyl group is thought to occlude the channel pore by projecting into the selectivity filter. During channel activation, the carboxyl group would be displaced out of the filter to allow ion conduction. Dutzler *et al.* (2003) suggested that extracellular Cl^- and H^+ activate bacterial ClC channels by displacing the residue. To support their model, Dutzler *et al.* (2003) demonstrated that mutation of the corresponding glutamate residue in ClC-0 causes constitutive channel activation.

Interestingly, Dutzler *et al.* (2002) showed that the α-helix that immediately precedes the intracellular C-terminus of bacterial ClC channels contributes directly to the coordination of Cl^- within the selectivity filter. They speculated that the C-terminus could provide a direct route for regulating channel activity by intracellular signalling events. Alignment of CLH-3 with the *Salmonella typhimurium* ClC channel revealed that the glutamate residue identified in the X-ray crystal structures is conserved in both splice variants. In addition, isoleucine, phenylalanine, serine and tyrosine residues, which are thought to function in Cl^- binding within the bacterial ClC channel pore (Dutzler *et al.* 2002), are also conserved. If these conserved residues are involved in ion conduction and activation of CLH-3, the different sensitivities of CLH-3a and CLH-3b to predepolarization, bath Cl^- and pH suggests that alternative splicing of the C-terminus may affect the accessibility and/or function of pore-associated ion binding sites. Recent electrophysiological studies carried out on oocytes that were isolated from a worm strain harbouring a deletion mutation in the CLH-3 C-terminus strongly support this idea (J. Denton & K. Strange, unpublished results). Detailed molecular analysis of CLH-3a and CLH-3b is clearly warranted to explore how C-terminal splice variation alters channel gating.

In addition to a role in regulating channel gating, it is intriguing to speculate that the unique C-terminus of CLH-3b may also play an important role in cell cycle signalling mechanisms. We have recently identified four proteins by yeast 2-hybrid analysis that interact with this region of the channel (J. Denton, K. Nehrke & K. Strange, unpublished results). Two of the four proteins may play well-established roles in cell cycle functions. A third protein is a component of a putative protein complex identified by large-scale protein–protein interaction mapping (Walhout *et al.* 2000). This protein complex includes two MAP kinases known to play essential roles in *C. elegans* meiotic cell cycle progression. Thus, the C-terminus of CLH-3b may function as a scaffold for proteins that regulate channel activity and/or other cell cycle-associated physiological processes.

Possible physiological roles of CLH-3 splice variants

The striking differences in their structure and biophysical properties suggest strongly that CLH-3 splice variants perform specific physiological roles in different cell types. GFP reporter studies have demonstrated that *clh-3* is transcriptionally expressed in the excretory cell, vulval cells, uterus, hermaphrodite-specific neurones (HSN), enteric muscles, and the first four epithelial cells of the intestine (Schriever *et al.* 1999; Nehrke *et al.* 2000). Schriever *et al.* (1999) suggested that depolarization-induced potentiation of CLH-3a (Figs 4 and 5) may play an important role in excitable cell function. For example, enteric muscles contract during the expulsion phase of the defecation cycle (Thomas, 1990; Liu & Thomas, 1994) and appear to be excited directly by the GABAergic motor neurones AVL and DVB (McIntire *et al.* 1993). These muscle cells express L-type Ca^{2+} channels that likely give rise to action potentials with relatively long-lived periods of depolarization (Lee *et al.* 1997). If CLH-3a is expressed in the enteric muscles, hyperpolarization-induced activation would be potentiated by prolonged depolarization (Figs 4 and 5). During repolarization, CLH-3a opening could conceivably function to correct overshoots in membrane voltage (see, for example, Davis *et al.* 1999).

In contrast to muscle cells, relatively little is known about the electrophysiological properties of specific types of *C. elegans* neurones. Goodman *et al.* (1998) developed a so-called 'slit worm preparation' where neurones are exposed by cutting a small slit in the animal's cuticle. These studies suggested that nematode neurones do not

exhibit classical rapid and repetitive action potentials and that instead they transmit electrical signals via a passive spread of membrane voltage. As in muscle cells, CLH-3a could function in neurones to correct overshoots in membrane voltage during repolarization. Interestingly, CLH-3 expression appears to be limited largely to the HSN, which innervate vulval muscles and control egg laying (Trent *et al.* 1983). No electrophysiological measurements have been carried out on the HSN, but it is conceivable that their electrophysiological properties differ from the neurones studied by Goodman *et al.* (1998) and may depend uniquely on CLH-3 activity.

As shown in the present study, CLH-3b is expressed in the oocyte (Fig. 12) and is probably responsible for the inwardly rectifying whole-cell current (e.g. Fig. 9). The physiological stimulus for activation of CLH-3b is initiation of oocyte meiotic maturation (Rutledge *et al.* 2001; Rutledge *et al.* 2002). Signals released from the maturing oocyte induce contractions in the surrounding smooth muscle-like sheath cells that drive the oocyte into the spermatheca (McCarter *et al.* 1999). Knockdown of *clh-3* expression by RNA_i disrupts the timing of sheath cell ovulatory contractions (Rutledge *et al.* 2001). We have suggested that activation of CLH-3 depolarizes the oocyte and electrically coupled sheath cells and that depolarization in turn modulates Ca^{2+} signalling pathways that control sheath contractility (Rutledge *et al.* 2001; Strange, 2002; Strange, 2003).

Depolarization-induced potentiation such as is observed with CLH-3a (Figs 4 and 5) would probably have no functional significance in the oocyte. Thus, expression of the CLH-3b splice variant may be restricted to oocytes and other nonexcitable cells such as the intestine and excretory cell. The primary function of CLH-3b in the oocyte may be to depolarize membrane potential. In the intestine and excretory cell, CLH-3b may function in transepithelial Cl^- transport. Immunolocalization of CLH-3a and CLH-3b expression patterns coupled with whole animal functional assays and electrophysiological studies in cultured *C. elegans* cells (Christensen *et al.* 2002) should help to elucidate the precise physiological roles of these splice variants.

In conclusion, we have shown that alternative splicing of the CLH-3 N- and C-termini has striking effects on the biophysical properties of this channel. Identification of the structural basis of these effects should provide new understanding of the molecular mechanisms of ClC gating and the role of intracellular domains in regulating ClC channel activity. Furthermore, the detailed characterization of CLH-3a and CLH-3b expression patterns and the physiology of CLH-3-expressing cells will likely yield novel insights into anion channel function and the role of splice variation in increasing ClC functional diversity.

References

Adrian RH & Bryant SH (1974). On the repetitive discharge in myotonic muscle fibres. *J Physiol* **240**, 505–515.

Arreola J, Begenisich T & Melvin JE (2002). Conformation-dependent regulation of inward rectifier chloride channel gating by extracellular protons. *J Physiol* **541**, 103–112.

Bargmann CI (1998). Neurobiology of the *Caenorhabditis elegans* genome. *Science* **282**, 2028–2033.

Brenner S (1974). The genetics of *Caenorhabditis elegans*. *Genetics* **77**, 71–94.

Chen TY & Miller C (1996). Nonequilibrium gating and voltage dependence of the ClC-0 Cl^- channel. *J General Physiol* **108**, 237–250.

Christensen M, Estevez AY, Yin XM, Fox R, Morrison R, McDonnell M, Gleason C, Miller DM & Strange K (2002). A primary culture system for functional analysis of *C. elegans* neurons and muscle cells. *Neuron* **33**, 503–514.

Cid LP, Niemeyer MI, Ramirez A & Sepulveda FV (2000). Splice variants of a ClC-2 chloride channel with differing functional characteristics. *Am J Physiol* **279**, C1198–C1210.

Davis MW, Fleischhauer R, Dent JA, Joho RH & Avery L (1999). A mutation in the *C. elegans* EXP-2 potassium channel that alters feeding behavior. *Science* **286**, 2501–2504.

Dutzler R, Campbell EB, Cadene M, Chait BT & MacKinnon R (2002). X-ray structure of a ClC chloride channel at 3.0 Å reveals the molecular basis of anion selectivity. *Nature* **415**, 287–294.

Dutzler R, Campbell EB & MacKinnon R (2003). Gating the selectivity filter in ClC chloride channels. *Science* **300**, 108–112.

Epstein HF & Shakes DC (eds.) (1995). *Caenorhabditis elegans: modern biological analysis of an organism (Methods in Cell Biology)* Volume 48 Academic Press, Inc. Orlando, FL, USA.

Ferroni S, Nobile M, Caprini M & Rapisarda C (2000). pH modulation of an inward rectifier chloride current in cultured rat cortical astrocytes. *Neuroscience* **100**, 431–438.

Fettiplace R & Fuchs PA (1999). Mechanisms of hair cell tuning. *Annu Rev Physiol* **61**, 809–834.

Fong P, Rehfeldt A & Jentsch TJ (1998). Determinants of slow gating in ClC-0, the voltage-gated chloride channel of *Torpedo marmorata*. *Am J Physiol* **274**, C966–C973.

Gaxiola RA, Yuan DS, Klausner RD & Fink GR (1998). The yeast CLC chloride channel functions in cation homeostasis. *Proc Natl Acad Sci USA* **95**, 4046–4050.

Geelen D, Lurin C, Bouchez D, Frachisse JM, Lelievre F, Courtial B, Barbier-Brygoo H & Maurel C (2000). Disruption of putative anion channel gene AtCLC-a in Arabidopsis suggests a role in the regulation of nitrate content. *Plant J* **21**, 259–267.

Goodman MB, Hall DH, Avery L & Lockery SR (1998). Active currents regulate sensitivity and dynamic range in *C. elegans* neurons. *Neuron* **20**, 763–772.

Gründer S, Thiemann A, Pusch M & Jentsch TJ (1992). Regions involved in the opening of CIC-2 chloride channel by voltage and cell volume. *Nature* **360**, 759–762.

Gunther W, Luchow A, Cluzeaud F, Vandewalle A & Jentsch TJ (1998). ClC-5, the chloride channel mutated in Dent's disease, colocalizes with the proton pump in endocytotically active kidney cells. *Proc Natl Acad Sci USA* **95**, 8075–8080.

Haug K, Warnstedt M, Alekov AK, Sander T, Ramirez A, Poser B, Maljevic S, Hebeisen S, Kubisch C, Rebstock J, Horvath S, Hallmann K, Dullinger JS, Rau B, Haverkamp F, Beyenburg S, Schulz H, Janz D, Giese B, Muller-Newen G, Propping P, Elger CE, Fahlke C, Lerche H & Heils A (2003). Mutations in CLCN2 encoding a voltage-gated chloride channel are associated with idiopathic generalized epilepsies. *Nat Genet* **33**, 527–532.

Hubbard EJ & Greenstein D (2000). The *Caenorhabditis elegans* gonad: a test tube for cell and developmental biology. *Dev Dyn* **218**, 2–22.

Iyer R, Iverson TM., Accardi A & Miller C (2002). A biological role for prokaryotic ClC chloride channels. *Nature* **419**, 715–718.

Jentsch TJ, Stein V, Weinreich F & Zdebik AA (2002). Molecular structure and physiological function of chloride channels. *Physiol Rev* **82**, 503–568.

Jordt SE & Jentsch TJ (1997). Molecular dissection of gating in the ClC-2 chloride channel. *EMBO J* **16**, 1582–1592.

Lee RY, Lobel L, Hengartner M, Horvitz HR & Avery L (1997). Mutations in the alpha1 subunit of an 1-type voltage-activated Ca^{2+} channel cause myotonia in *Caenorhabditis elegans*. *EMBO J* **16**, 6066–6076.

Lipscombe D, Pan JQ & Gray AC. (2002). Functional diversity in neuronal voltage-gated calcium channels by alternative splicing of Ca (v) alpha1. *Mol Neurobiol* **26**, 21–44.

Liu DW & Thomas JH (1994). Regulation of a periodic motor program in *C. elegans*. *J Neurosci* **14**, 1953–1962.

McCarter J, Bartlett B, Dang T & Schedl T (1999). On the control of oocyte meiotic maturation and ovulation in *Caenorhabditis elegans*. *Dev Biol* **205**, 111–128.

McIntire SL, Jorgensen E, Kaplan J & Horvitz HR (1993). The GABAergic nervous system of *Caenorhabditis elegans*. *Nature* **364**, 337–341.

Mohammad-Panah R, Harrison R, Dhani S, Ackerley C, Huan LJ, Wang Y & Bear CE (2003). The chloride channel ClC-4 contributes to endosomal acidification and trafficking. *J Biol Chem* **278**, 29267–29277.

Nehrke K, Begenisich T, Pilato J & Melvin JE (2000). *C. elegans* ClC-type chloride channels: novel variants and functional expression. *Am J Physiol* **279**, C2052–C2066.

Pusch M (2002). Myotonia caused by mutations in the muscle chloride channel gene CLCN1. *Hum Mutat* **19**, 423–434.

Rutledge E, Bianchi L, Christensen M, Boehmer C, Morrison R, Broslat A, Beld AM, George A, Greenstein D & Strange K (2001). CLH-3, a ClC-2 anion channel ortholog activated during meiotic maturation in *C. elegans* oocytes. *Curr Biol* **11**, 161–170.

Rutledge E, Denton J & Strange K (2002). Cell cycle- and swelling-induced activation of a *Caenorhabditis elegans* ClC channel is mediated by CeGLC-7α/β phosphatases. *J Cell Biol* **158**, 435–444.

Rychkov GY, Astill DS, Bennetts B, Hughes BP, Bretag AH & Roberts ML (1997). pH-dependent interactions of Cd^{2+} and a carboxylate blocker with the rat C1C-1 chloride channel and its R304E mutant in the Sf-9 insect cell line. *J Physiol* **501**, 355–362.

Rychkov GY, Pusch M, Astill DS, Roberts ML, Jentsch TJ & Bretag AH (1996). Concentration and pH dependence of skeletal muscle chloride channel ClC-1. *J Physiol* **497**, 423–435.

Schriever AM, Friedrich T, Pusch M & Jentsch TJ (1999). CLC chloride channels in *Caenorhabditis elegans*. *J Biol Chem* **274**, 34238–34244.

Shimada K, Li X, Xu G, Nowak, DE, Showalter, LA & Weinman, SA (2000). Expression and canalicular localization of two isoforms of the ClC-3 chloride channel from rat hepatocytes. *Am J Physiol* **279**, G268–G276.

Staley K, Smith R, Schaack J, Wilcox C & Jentsch TJ (1996). Alteration of GABAA receptor function following gene transfer of the CLC-2 chloride channel. *Neuron* **17**, 543–551.

Strange K (2002). Of mice and worms: novel insights into ClC-2 anion channel physiology. *News Physiol Sci* **17**, 11–16.

Strange K (2003). From genes to integrative physiology: ion channel and transporter biology in *Caenorhabditis elegans*. *Physiol Rev* **83**, 377–415.

Thomas JH (1990). Genetic analysis of defecation in *Caenorhabditis elegans*. *Genetics* **124**, 855–872.

Trent C, Tsuing N & Horvitz HR (1983). Egg-laying defective mutants of the nematode *Caenorhabditis elegans*. *Genetics* **104**, 619–647.

Uchida S (2000). *In vivo* role of CLC chloride channels in the kidney. *Am J Physiol* **279**, F802–F808.

Varela D, Niemeyer MI, Cid LP & Sepulveda FV (2002). Effect of an N-terminus deletion on voltage-dependent gating of the ClC-2 chloride channel. *J Physiol* **544**, 363–372.

Walhout AJ, Sordella R, Lu X, Hartley JL, Temple GF, Brasch MA, Thierry-Mieg N & Vidal M (2000). Protein interaction mapping in *C. elegans* using proteins involved in vulval development. *Science* **287**, 116–122.

Zagotta WN, Hoshi T & Aldrich RW (1990). Restoration of inactivation in mutants of Shaker potassium channels by a peptide derived from ShB. *Science* **250**, 568–571.

Acknowledgments

This work was supported by NIH grant R01 DK51610 to K.S., by NIH National Research Service Award *f*32 G067424.01 and NIH training grant T32 NS07491 to J.D., and by NIH grant R21 DK062763 to K.N. The *clh-3(ok763)* worms were provided by the *C. elegans* Gene Knockout Project at OMRF, which is part of the International *C. elegans* Gene Knockout Consortium (*http://www.mutantfactory.ouhsc.edu/*).

Author's present address

E. Rutledge: Department of Biology, Skidmore College, Saratoga Springs, NY 12866, USA.